Journal of Inorganic Biochemistry 143 (2015) 56–63

Contents lists available at ScienceDirect

Journal of Inorganic Biochemistry

journal homepage: www.elsevier.com/locate/jinorgbio

Effect of ancillary ligands on the interaction of ruthenium(II) complexes with the triplex RNA poly(U)·poly(A)*poly(U)

Jia Li [a,1], Yanmei Sun [a,1], Lingjun Xie [a], Xiaojun He [a], Lifeng Tan [b,*]

[a] College of Chemistry, Xiangtan University, Xiangtan, PR China
[b] Key Lab of Environment-friendly Chemistry and Application in Ministry of Education, Xiangtan University, Xiangtan, PR China

ARTICLE INFO

Article history:
Received 5 September 2014
Received in revised form 3 December 2014
Accepted 3 December 2014
Available online 11 December 2014

Keywords:
Ru(II) complexes
Triplex RNA
Interaction
Stabilization

ABSTRACT

Two new Ru(II) complexes with 1,8-naphthalimide group, $[Ru(phen)_2(pnip)]^{2+}$ (Ru**1**; phen = 1,10-phenanthroline, pnip = 2-[*N*-(*p*-phenyl)-1,8-napthalimide]imidazo[4′,5′-*f*][1,10]phenanthroline) and $[Ru(bpy)_2(pnip)]^{2+}$ (Ru**2**; bpy = 2,2′-bipyridine), have been synthesized and characterized. The interactions of Ru**1** and Ru**2** with the triplex RNA poly(U)•poly(A)*poly(U) (where • denotes the Watson–Crick base pairing and * denotes the Hoogsteen base pairing) were studied by various biophysical. Electronic spectra established that the binding affinity for Ru**1** was greater than that for Ru**2**. Fluorescence and viscosity studies gave convincing evidence for a true intercalative binding of both complexes with the RNA triplex. UV melting studies confirmed that the two complexes could stabilize the triplex, whereas the effects of the two complexes on the stability of the Hoogsteen base-paired strand ploy(U) and the Watson–Crick base-paired duplex poly(U)•poly(A) of the triplex were different. In the case of Ru**1**, the increase of the thermal stability of the Hoogsteen base-paired strand was stronger than that of the Watson–Crick base-paired duplex. However, an opposite effect was observed in the case of Ru**2**. Circular dichroic studies suggested that the RNA triplex undergoes a conformational transition in the presence of Ru**1**, whereas the helicity of the RNA triplex still remains A-type in the presence of Ru**2**. The main results obtained here further advance our knowledge on the interaction of RNA triple-stranded structures with metal complexes, particularly ruthenium(II) complexes.

1. Introduction

Nucleic acid triple-stranded structures, also called triplexes, are complexes of three oligonucleotide strands made from either RNA or DNA [1–3]. Over the last decades, there is renewed interest in investigating triplex nucleic acids because triplexes may be implicated in a range of cellular functions, such as transcriptional regulation, post-transcriptional RNA processing and modification of chromatin [4,5]. However, due to the Hoogsteen base pairing, the stability of triplexes is much lower than that of the corresponding duplex, which hinders the practical applications of triplexes [6,7]. In this regard, small molecules able to recognize, bind and stabilize the specific sequences of the triple helical nucleic acid structures are of very importance.

In recent years, many natural and synthetic compounds able to enhance the stability of triplexes have been reported [8–10]. In contrast to DNA triplexes, investigations of small molecules effect on the stabilization of RNA triplexes at present are mainly limited to organic compounds [11–13] and, to a far lesser extent, on metal complexes [14–16]. Previous reports indicate that the stabilization of RNA triplexes can be achieved by the action of intercalators [17,18], in particular when covalently linked to the third strand [19]. However, intercalators not covalently linked can either stabilize or destabilize RNA triplexes [20,21]. For example, the melting experiments reveal that proflavine (PR) and its platinum(II)-proflavine complex PtPR [14] (Fig. 1) and ethidium [22] tend to destabilize the triplex, whereas berberine analogs [12] are able to strongly stabilize the Hoogsteen base-paired third strand of the triplex by intercalation. Interestingly, some alkaloids stabilize the Hoogsteen base-paired third strand of the triplex almost without affecting the stability of the duplex, such as berberine, palmatine and coralyne [17]. These studies reveal that the binding processes and modes effect on the stability of RNA triplexes are more complicated than previously thought. Recently, we reported the recognition of triplex RNA structures by Ru(II) complex, $[Ru(phen)_2(mdpz)]^{2+}$ [15]. The results indicate that this intercalator can enhance the stability of the triplex RNA poly(U)•poly(A)*poly(U) and act as a first emission 'light switch' for this triplex.

It is well established that Ru(II) polypyridyl complexes, due to a combination of easily constructed rigid chiral structures spanning all three spatial dimensions and a rich photophysical repertoire, prominent DNA binding properties and promising biological activity, have attracted considerable attentions in recent years [23–25]. However, the interactions of Ru(II) polypyridyl complexes between RNA triplexes

* Corresponding author at: College of Chemistry, Xiangtan University, Xiangtan 411105, PR China. Tel.: +86 731 58293997; fax: +86 731 58292477.
E-mail address: lfwyxh@yeah.net (L. Tan).
[1] These two authors are both first authors.

http://dx.doi.org/10.1016/j.jinorgbio.2014.12.007
0162-0134/

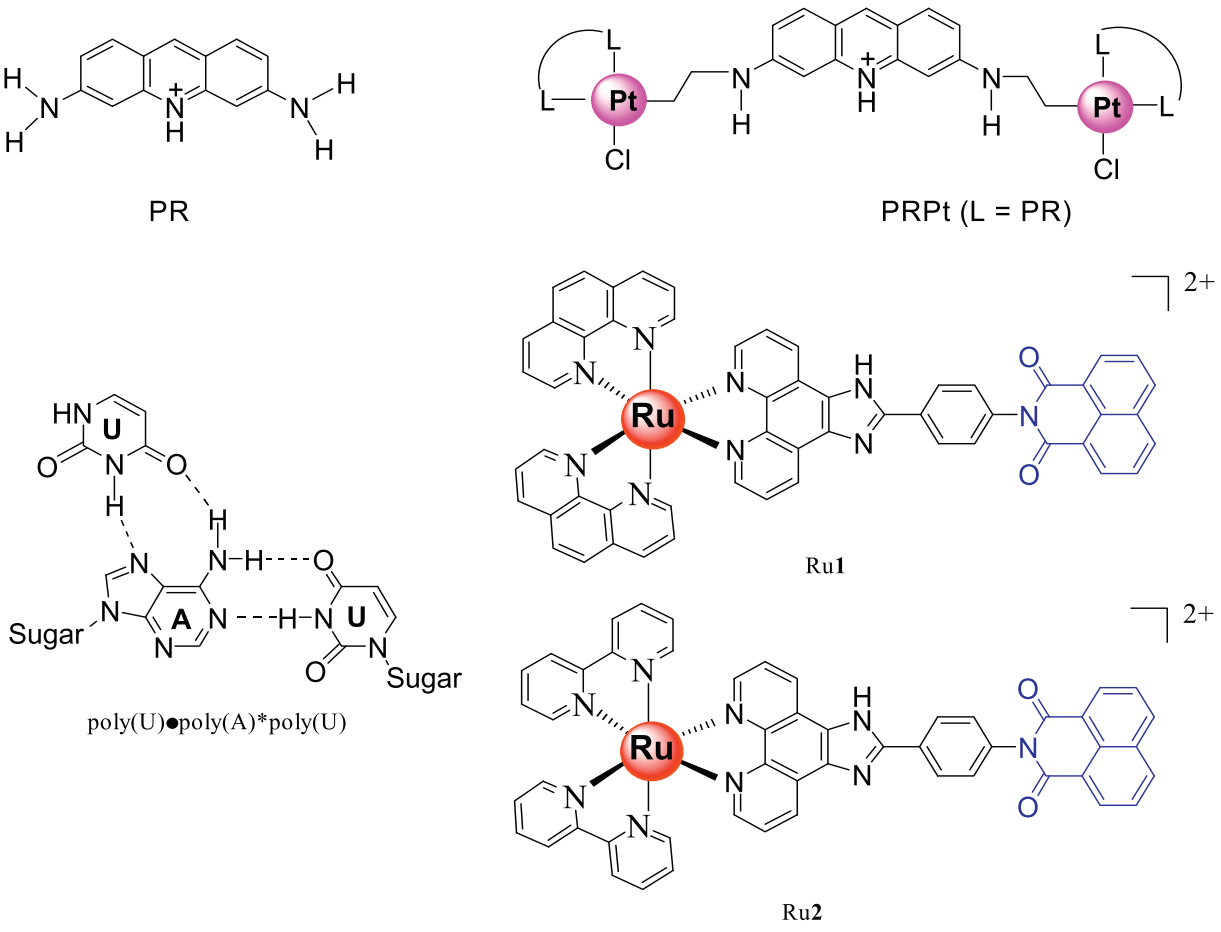

Fig. 1. Chemical structures of PR, PtPR, Ru**1**, Ru**2** and the base pairing scheme in poly(U)•poly(A)*poly(U) (symbols • and * represent Watson–Crick and Hoogsteen base pairing).

have attracted a spot of front attention [14,15]. To more clearly evaluate and understand the factors effect on the stability of RNA triplexes, further studies using Ru(II) polypyridyl complexes with different shapes and electronic properties are quite significant and necessary.

In addition, we note that 1,8-naphthalimide and its derivatives have received significant attention during the past two decades because of their excellent photophysical properties and defined structure [26–28]. Furthermore, these compounds are known to be effective binders and photoreactive reagents for DNA [29,30]. With this in mind, a novel polypyridyl ligand with 1,8-naphthalimide group and its Ru(II) complexes (Fig. 1), $[Ru(phen)_2(pnip)]^{2+}$ (Ru**1**; phen = 1,10-phenanthroline, pnip = 2-[*N*-(*p*-phenyl)-1,8-napthalimide]imidazo[4',5'-*f*][1,10]phenanthroline) and $[Ru(bpy)_2(pnip)]^{2+}$ (Ru**2**; bpy = 2,2′-bipyridine), have been synthesized and characterized. The interactions of the two Ru(II) complexes with the RNA triplex poly(U)•poly(A)*poly(U) (where • denotes the Watson–Crick base pairing and * denotes the Hoogsteen base pairing; Fig. 1) was investigated by various biophysical techniques. To the best of our knowledge, Ru**1** and Ru**2** are the first examples of Ru(II) polypyridyl complexes with 1,8-naphthalimide group as triplex RNA binders.

2. Experimental sections

2.1. Materials

1,10-Phenanthroline-5,6-dione [31], 2-(4-aminophenyl)imidazo[4,5-*f*][1,10]phenanthroline (paip) [32], *cis*-$[Ru(phen)_2Cl_2]\cdot 2H_2O$, and *cis*-$[Ru(bpy)_2Cl_2]\cdot 2H_2O$ [33] were prepared according to literature procedures. Polynucleotide samples of double-stranded poly(A)•poly(U) and single-stranded poly(U) were obtained from Sigma-Aldrich Corporation (St. Louis, MO, USA) and were used as received. The RNA triplex poly(U)·poly(A)*poly(U) was prepared as reported earlier [15]. The concentration of poly(U)·poly(A)*poly(U) was determined optically using molar absorption coefficient, ε (M^{-1} cm^{-1}) reported in the literature [34–36]. All titration experiments were conducted at 20 °C in pH 7.0 phosphate buffer (6 mmol/L Na_2HPO_4, 2 mmol/L NaH_2PO_4, 1 mmol/L Na_2EDTA, 19 mmol/L NaC1).

2.2. Physical measurement

Microanalyses (C, H and N) were carried out on a Perkin-Elmer 240Q elemental analyzer. ^1H NMR spectra were recorded on an Avance-400 spectrometer with d_6-DMSO as solvent at room temperature and TMS (tetramethylsilane) as the internal standard. Mass Spectrometer was performed on an Autoflex III™ MALDI-TOF-MS (matrix assisted laser desorption ionization time-of-flight mass spectrometry) (Bruker) using DMSO as the mobile phase. UV-visible (UV-vis) spectra were recorded on a Perkin-Elmer Lambda-25 spectrophotometer, and emission spectra were recorded on a Perkin-Elmer LS-55 luminescence spectrometer at room temperature. Circular dichroism (CD) spectra were measured on a JASCO-810 spectropolarimeter.

2.3. Synthesis of the ligand pnip

A mixture of paip (168 mg, 0.54 mmol), 1,8-naphthalic anhydride (106 mg, 0.54 mmol), and acetic acid (HAc, 15 mL) was heated at 120 °C for 5 h. The cooled solution was diluted with H_2O and neutralized with concentrated $NH_3\cdot H_2O$. The brown precipitate was collected and purified by chromatography on a neutral alumina column with ethanol-toluene (5:1, v/v) as the eluant to give the title compound as

an amorphous brown solid. Yield, 201 mg (78%). Anal (%). Cal. for $C_{31}H_{17}N_5O_4 \cdot H_2O$: C, 73.08; H, 3.76; N, 13.74. Found: C, 72.97; H, 3.82; N, 13.69. MALDI-TOF-MS (*m/z*): 492.2 [M + 1].

2.4. Synthesis of $[Ru(phen)_2(pnip)](ClO_4)_2 \cdot H_2O$ (Ru1)

A mixture of *cis*-$[Ru(phen)_2Cl_2]\cdot 2H_2O$ (130 mg, 0.25 mmol), pnip (123 mg, 0.25 mmol) and ethylene glycol (20 mL) was thoroughly deoxygenated. The purple mixture was heated for 8 h at 150 °C under argon. When the solution finally turned reddish brown, it was cooled to room temperature, and equal volume of saturated aqueous sodium perchlorate solution was added under vigorous stirring. The brownish solid was collected and washed with small amounts of water, ethanol and diethyl ether, respectively, and then dried under vacuum and purified on a neutral alumina column with MeCN–toluene (4:1, v/v) as eluant. Yield: 59%. Anal (%). Cal. for $C_{55}H_{33}N_9Cl_2O_{10}Ru \cdot H_2O$: C, 56.47; H, 3.02; N, 10.78. Found: C, 56.41; H, 3.17; N, 10.80. λ_{max}/nm (ε/M^{-1} cm^{-1}, MeCN): 459 (19745), 288 (99350). ^{1}H NMR (400 MHz, ppm, d_6-DMSO; d, doublet; s, singlet; t, triplet; m, multiplet): 14.38 (s, 1H), 10.26 (s, 2H), 9.12 (s, 2H), 8.76 (d, 4H, J = 8.0 Hz), 8.56 (dd, 4H, J_1 = 2.4 Hz, J_2 = 1.2 Hz), 8.25 (d, 4H, J = 8.4 Hz), 8.08 (d, J = 21.6 Hz, 4H), 7.89 (d, J = 28.8 Hz, 6H), 7.60 (s, 4H), 7.92 (s, 2H), 7.35 (s, 2H). MALDI-TOF-MS (*m/z*): 952.8 ($[M–2ClO_4–H]^+$).

2.5. Synthesis of $[Ru(bpy)_2(pnip)](ClO_4)_2 \cdot H_2O$ (Ru2)

The brownish complex $[Ru(bpy)_2(pnip)]^{2+}$ was obtained by a similar procedure to that described above. Yield: 64%. Anal (%). Cal. for $C_{51}H_{33}N_9Cl_2O_{10}Ru \cdot H_2O$: C, 54.60; H, 3.14; N, 11.24. Found: C, 54.57; H, 3.22; N, 11.36. λ_{max}/nm (ε/M^{-1} cm^{-1}, MeCN): 458 (17530), 288 (53610), 264 (80550). ^{1}H NMR (400 MHz, ppm, D_6-DMSO; d, doublet; s, singlet; t, triplet; m, multiplet): 14.39 (s, 1H), 9.12 (s, 2H), 8.89 (d, 4H, J = 8.4 Hz), 8.85 (d, 2H, J = 8.0 Hz), 8.57 (d, 2H, J = 8.0 Hz), 8.28 (d, 2H, J = 8.4 Hz), 8.24 (t, 4H, J_1 = 7.6 Hz, J_2 = 14.0 Hz), 8.13 (d, 4H, J = 21.6 Hz), 8.06 (d, 2H, J = 4.8 Hz), 7.92 (s, 2H), 7.86 (d, 4H, J = 6.0 Hz), 7.61 (s, 4H), 7.36 (s, 2H). MALDI-TOF-MS (*m/z*): 904.1($[M–2ClO_4–H]^+$).

Caution: Perchlorate salts of compounds containing organic ligands are potentially explosive. Small quantities should be prepared and handled with care.

2.6. RNA-binding experiments

The methods for spectroscopic titrations and viscosity measurements of Ru**1** and Ru**2** binding with poly(U).poly(A)*poly(U) have already been described [15]. The intrinsic binding constants (K_b) and the binding sites (s) are determined the changes of MLCT (MLCT = metal to ligand charge transfer) bands at 458 nm for Ru**1** and 456 nm for Ru**2** by using the following equation [37]:

$$\frac{\varepsilon_a-\varepsilon_f}{\varepsilon_b-\varepsilon_f}=\frac{\sqrt{b-(b^2-2K_b^2C_t[RNA]/s)}}{2K_bC_t} \quad (1a)$$

$$b=\frac{1+K_bC_t+K_b[RNA]}{2s} \quad (1b)$$

where [RNA] is the concentration of poly(U)·poly(A)*poly(U) in the nucleotide phosphate and ε_a, ε_f and ε_b are the apparent, free and bound metal complex extinction coefficients, respectively. K_b is the equilibrium binding constant in M^{-1}, C_t is the total metal complex concentration and s is the binding site size.

2.7. Thermal denaturation studies

Thermal poly(U)·poly(A)*poly(U) denaturation experiments were carried out with a Perkin-Elmer Lambda-25 spectrophotometer equipped with a Peltier temperature-control programmer (±0.1 °C). The temperature of the solution was increased from 20 to 60 °C at a rate of 1 °C min^{-1}, and the absorbance at 260 nm was continuously monitored for solutions of the RNA triplex (32.1 μM) with different concentrations of either Ru**1** or Ru**2** in phosphate buffer. The thermal melting temperature (T_m) was taken as the midpoint of the melting transition as determined by the maximal of the first derivative plot [14].

3. Results and discussion

3.1. Synthesis and characterization

The synthetic routes to the ligand pnip and its complexes Ru**1** and Ru**2** is shown in Scheme 1.

Ligand pnip was prepared by the reaction of paip with 1,8-naphthalic anhydride in glacial acetic acid according to literature methods [31]. Using ethylene glycol as solvent, Ru**1** and Ru**2** were prepared by direct the reaction of either *cis*-$[Ru(phen)_2Cl_2]\cdot 2H_2O$ or *cis*-$[Ru(phen)_2Cl_2]\cdot 2H_2O$ with the appropriate mole ratios of pnip, and obtained in yields of 59% and 61%, respectively. The desired Ru(II) complexes were isolated as their hexafluorophosphates and then purified by column chromatography. Both complexes were characterized by elemental analysis, mass spectroscopy and NMR spectroscopy. In the Maldi-Tof mass spectra of Ru**1** or Ru**2**, one signal of ($[M–2ClO_4–H]^+$ was observed and the determined molecular weights were consistent with the expected value.

Ru**1** and Ru**2** give well-defined ^{1}H NMR spectra (Fig. 2), which further permit unambiguous identification and assessment of their purity. In comparison to those of similar compounds [31], the proton chemical shifts were assigned by allowing for the influence of the steric, inductive and conjugative effects. For each of the complexes, two sets of NMR signals were observed. Because of the shielding influences of the adjacent pnip and phen (or bpy) moieties, the two halves of each phen (or bpy) are not chemically and magnetically equivalent, which leads to eight signals that correspond to the phen (or bpy) protons: one set of four is associated with the bpy (or phen) half near the ligand pnip and the other set of four is associated with the phen (or bpy) portion near the other phen (or bpy). Since the shielding effect of pnip is obviously greater than that of phen (or bpy), the chemical shifts of the latter protons appear more downfield than those of the former. In general, it is difficult to observe the proton resonance on the nitrogen atom of the imidazole, due to the proton exchanging quickly between the two nitrogens of the imidazole ring [38,39]. However, for Ru**2**, the proton resonance on the nitrogen atom of the imidazole ring was observed at about 14.37 ppm indeed, indicating that this proton on the imidazole in Ru**2** is more active than that in Ru**1**.

3.2. Spectral properties

The characteristic absorbance spectra of Ru**1** and Ru**2**, along with their emission spectra, are shown in Fig. 3 and 4, respectively. For Ru**2**, the absorption spectrum (Fig. 3) showed a distinct band centered at 263 nm characteristic of intraligand π → π* transition [40] and an MLCT band at 456 nm, while for Ru**1**, the IL and MLCT bands displaying bathochromic shift centered at 289 and 458 nm, respectively. Exciting Ru**1** at 458 nm results in an MLCT emission centered at 609 nm, whereas Ru**2** excited at 456 nm shows an MLCT emission centered at 600 nm (Fig. 4). In addition, the emission intensity of Ru**1** is stronger than that of Ru**2** under the same condition. These suggest the ancillary ligands (phen and bpy) have significant effects on the spectral properties of Ru**1** and Ru**2**.

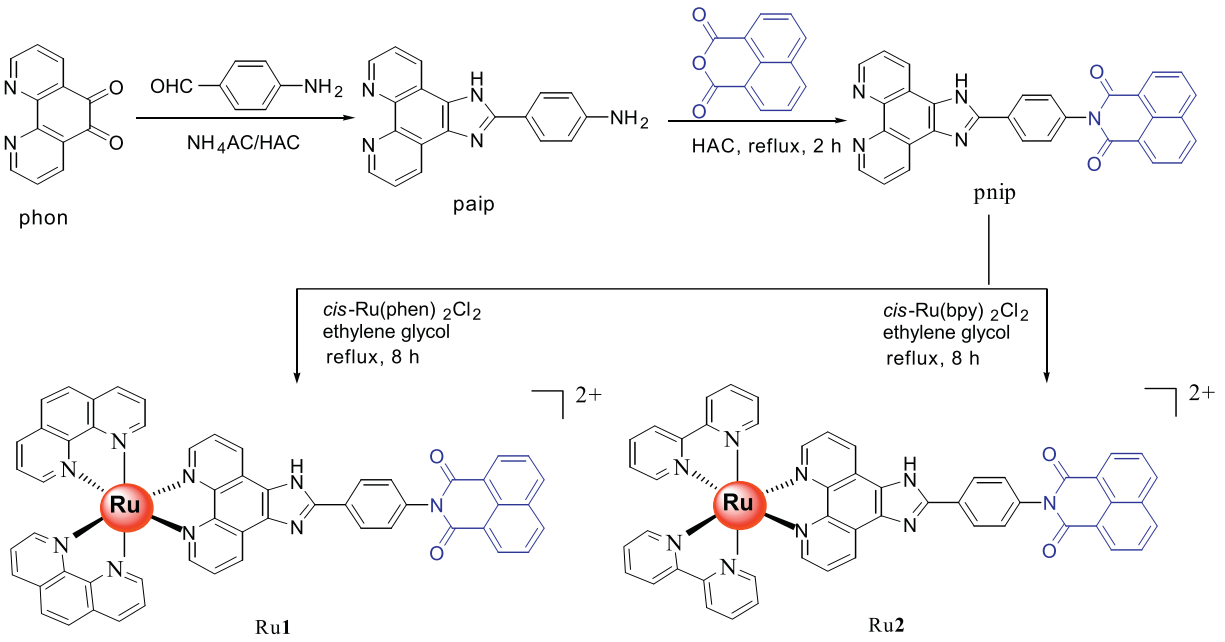

Scheme 1. Synthetic routes to the ligand pnip and its complexes Ru**1** and Ru**2**.

3.3. Electronic absorption spectral studies of the binding

Electronic absorption spectroscopy is one of the most useful techniques in triplexes-binding studies. Hypochromism and bathochroism are usually observed when complexes bind with triplexes through intercalation, due to the strong stacking interaction between an aromatic chromophore and the triplexes base pairs [41]. In general, the extent of hypochromism reflects the binding affinity. Thus, the bindings of Ru**1** and Ru**2** to the triplex RNA poly(U)•poly(A)*poly(U) are performed by UV-vis absorption spectra. The absorption spectroscopy changes of either Ru**1** or Ru**2** (at constant concentrations of complex) upon addition of the triplex RNA are shown in Fig. 5, and the representing data are listed in Table 1. Increasing the RNA concentration, and thus the [UAU]/[Ru] ratio (UAU stands for poly(U)•poly(A)*poly(U), Ru stands for Ru**1** or Ru**2**), results in different hypochromic and bathochromic effects for each complex. For Ru**1**, the MLCT band at 458 nm exhibited a 18% hypochromism with a red shift of 10 nm at [UAU]/[Ru**1**] ≈ 6.7. For Ru**2**, the MLCT band at 456 nm exhibited a 16% hypochromism

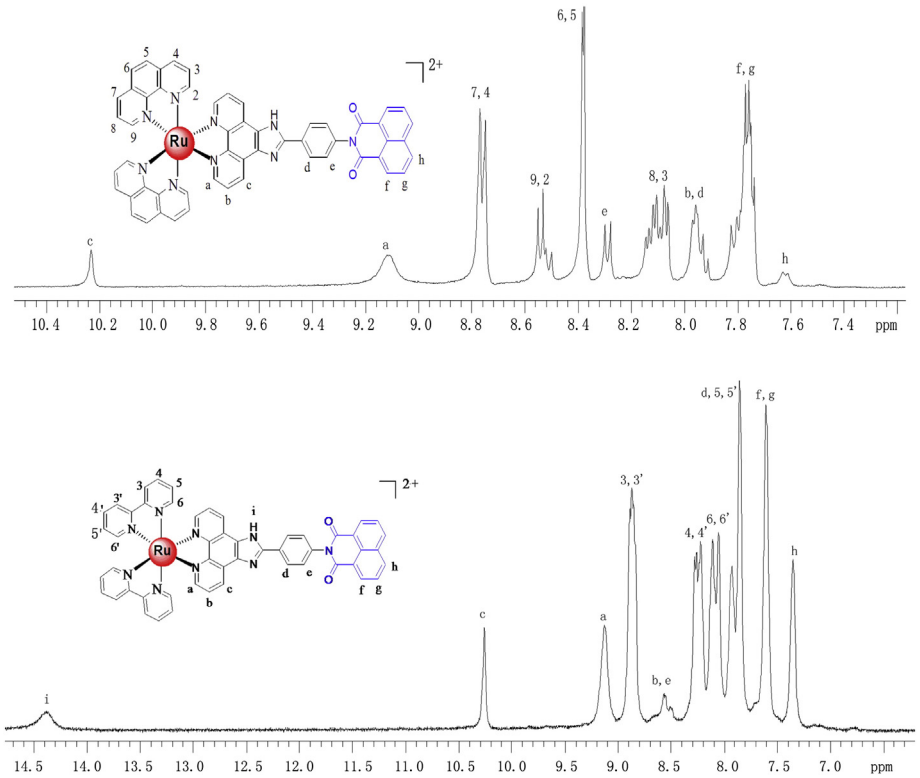

Fig. 2. ^{1}H NMR (400 MHz) of Ru**1** and Ru**2** in D_6-DMSO.

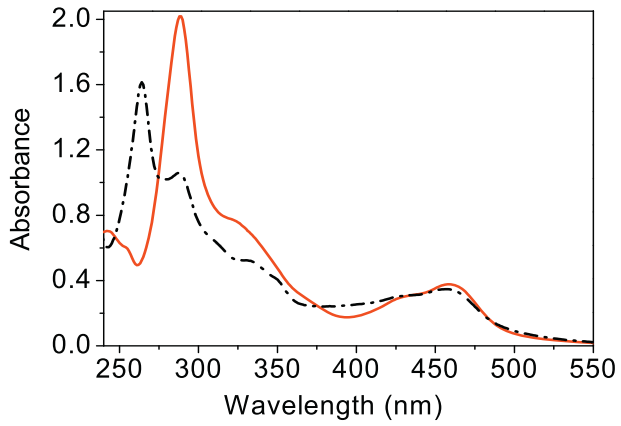

Fig. 3. UV–vis spectra of 20 μM Ru**1** ((red solid line) and Ru**2** (black dashed line) in CH_3CN.

with a red shift of 8 nm at [UAU]/[Ru**2**] ≈ 3.5. These absorption changes obviously indicate the binding of Ru**1** and Ru**2** to the RNA; the important hypochromic and the bathochromic effects would indicate intercalation of the pnip ligand between the base pairs of the RNA triplex helix. Interestingly, Fig. 5 and Table 1 indicate that hypochromicity is the most important for the LC pnip π → π* transitions. This is also in agreement with the intercalation of the ligand between the stacking of bases. The extent of hypochromicity is attributed to closely bound metal complexes. In addition, both the polarity effects of the triplex and electron transfer from the triplex base pairs may also contribute to the spectral changes of the two Ru(II) complexes to a certain extent. Finally, the carbonyl groups of the main ligand pnip and the oxygen or nitrogen components of the bases as well as of the neighboring phosphate groups of the triplex may form intermolecular hydrogen-bonds, which can also increase the binding strength of the two complexes toward the triplex.

To compare quantitatively the binding strength of the two complexes, the binding constant (K_b) and binding site size (n) are determined to be $(4.6 \pm 0.77) \times 10^6\ M^{-1}$ and 0.90 ± 0.01 for Ru**1** and $(2.5 \pm 0.87) \times 10^6\ M^{-1}$ and 0.40 ± 0.01 for Ru**2**, respectively. For Ru**1**, the values of K_b and n are slightly higher than those for Ru**2**. These suggest that the binding of Ru**1** with the RNA is tighter than that of Ru**2** with the RNA, which may be due to the effects of the ancillary ligands. Ongoing from bpy to phen, the plane area and hydrophobicity increase. Better planarity and greater hydrophobicity is more advantageous to the π-π stacking interaction between Ru**1** and the triplex RNA, which makes Ru**1** insert the bases of the triplex more deeply than Ru**2**, leading to a greater binding affinity for Ru**1**. In addition, the K_b values of the two complexes have the same order of magnitude to that of the known triplex RNA intercalator coralyne {$(4.0 \pm 0.60) \times 10^6\ M^{-1}$} [17]. Notably, the K_b values of the two complexes

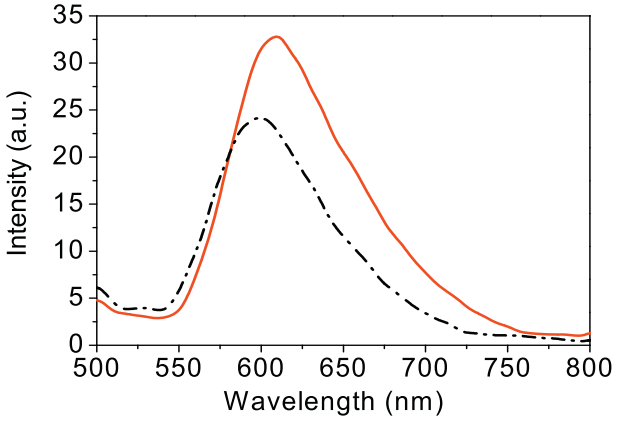

Fig. 4. Emission spectra of 2 μM Ru**1** ((red solid line) and Ru**2** (black dashed line) in CH_3CN.

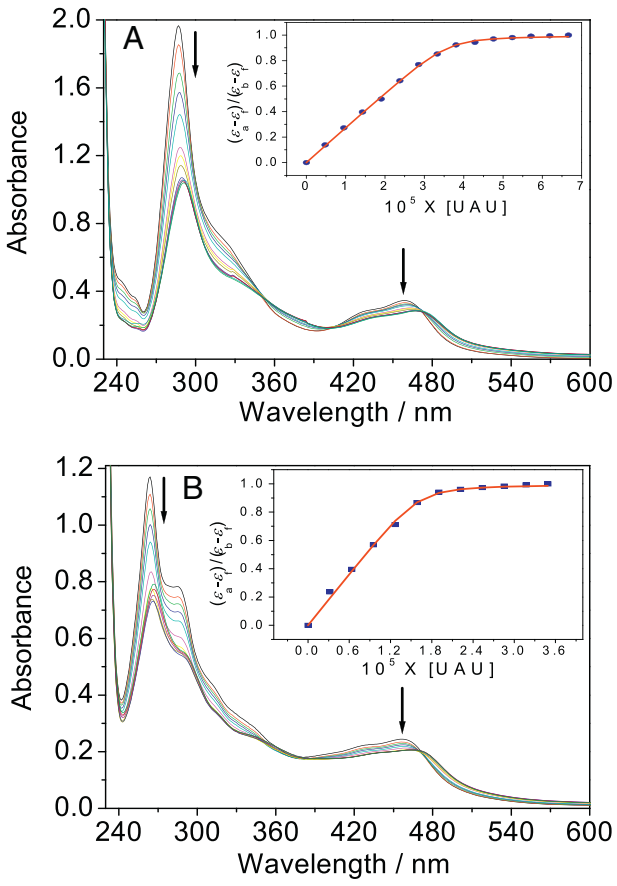

Fig. 5. Representative UV–vis spectral changes of Ru**1** (A) and Ru**2** (B) in the presence of poly(U)•poly(A)*poly(U) in phosphate buffer (6 mmol/L Na_2HPO_4, 2 mmol/L NaH_2PO_4, 1 mmol/L Na_2EDTA, 19 mmol/L NaC1, pH 7.0) at 20 °C. [Ru**1**] = [Ru**2**] = 20 μM, [UAU] = 0–67 μM, where UAU stands for the poly(U)·poly(A)*poly(U). The arrows show the absorbance change upon an increasing poly(U)·poly(A)*poly(U) concentration. Insert: plots of plotting $(\varepsilon_a - \varepsilon_b) / (\varepsilon_f - \varepsilon_b)$ *vs.* [UAU] and the nonlinear fit.

are much higher than those of the compounds binding with the triplex RNA through a partial intercalation, such as the metal complex PRPt $(1.3 \times 10^4\ M^{-1})$ [14], alkaloid berberine $(1.6 \pm 0.40) \times 10^5\ M^{-1}$) [17] and palmatine ($(1.6 \pm 0.40) \times 10^5\ M^{-1}$) [28], suggesting that the binding modes for Ru**1** and Ru**2** are likely intercalation. In addition, the binding site sizes (n) are smaller than 1, which may be indicative of a groove-binding nature for Ru**1** and Ru**2**.

3.4. Spectrofluorimetric studies of the binding

Ru**1** and Ru**2** can emit in the phosphate buffer with a maximum at about 600 nm. Moreover, when the luminescence of either Ru**1** or Ru**2** is measured at a constant complex concentration as a function of increasing amount of the RNA, the ratio I/I_0 (I and I_0 are the intensities in the presence and absence of the RNA, respectively) increases until a plateau value is reached (Fig. 6). For Ru**1**, its luminescence intensity increases about 2.4 times at [UAU]/[Ru**1**] ≈ 13.0, whereas for Ru**2**, whose luminescence intensity increases only 1.7 times at [UAU]/[Ru**1**] ≈ 8.3. A larger fluorescence change is indicative of a stronger association of Ru**1** to the RNA, resulting presumably from a more effective overlap of the bound Ru**1** with the base pairing of the RNA. The result also proposes the location of the bound complexes in a hydrophobic environment similar to an intercalated state and Ru**1** protected by the RNA is more efficient compared with Ru**2** [17]. In that case, the accessibility of water molecules to Ru**1** in the presence of the RNA is more difficult in comparison with Ru**2**. Therefore, Ru**1** displays a greater emission increase than Ru**2** upon binding with the triplex in saturation state.

Table 1
Binding constants (K_b), average binding site size (s), hypochromicity (H) and bathochromic shifts of Ru**1** and Ru**2**.

Title	$\lambda_{max,\ free}$ (nm)	$\lambda_{max,\ bound}$ (nm)	$\Delta\lambda$ (nm)[a]	H[b] (%)	K_b[c] ($\times 10^6\ M^{-1}$)	s[d]
Ru**1**	265	270	5	48	–	–
	458	468	10	18	4.6 ± 0.77	0.90 ± 0.01
Ru**2**	263	265	2	37	–	–
	456	464	8	16	2.5 ± 0.87	0.40 ± 0.08

[a] $\Delta\lambda$ represents the difference in wavelength of the IL and MLCT band of the metal complex between free and completely bound DNA states.
[b] $H = 100 \times (A_{free} - A_{bound}) / A_{free}$ (A is the absorbance).
[c] K_b was determined by monitoring the changes of absorption at the IL and MLCT bands.
[d] s is an average binding size.

3.5. Thermal denaturation studies

The thermal melting experiment is an effective method to investigate the interaction of small molecules with nucleic acids [42]. In general, the stacking interactions of intercalated molecules as well as the neutralization of the phosphate charges through external binding together may contribute to the enhancement of the melting temperature. Denaturation of a triplex nucleic acid into a duplex and a single strand leads to significant hyperchromism at around 260 nm. In particular, the specificity of the binding of a small molecule to either the Hoogsteen base-paired third strand or to the Watson–Crick base-paired duplex of triplexes can be easily discriminated.

The denaturation curves of the RAN triplex poly(U)•poly(A)*poly(U) in the absence and presence of each Ru(II) complexes are presented in Fig. 7, and the quantitative data on the melting temperatures at various [UAU]/[Ru] are summarized in Table 2. The RNA triplex alone melts in two well-resolved sequential transitions: the first separation from the triplex occurs at about 35.1 °C (T_{m1}) corresponding to the dissociation of the triplex into a poly(U)•poly(A) duplex and a poly(U) single strand; the second separation occurs at about 47.5 °C (T_{m2}), corresponding to the denaturation of the duplex poly(U)•poly(A) into its component single strands [39]. Fig. 7 and Table 2 indicate that the two Ru(II) complexes could enhance the triplex dissociation temperature. For Ru**1**, the values of ΔT_{m1} and ΔT_{m2} are about 10.5 and 9.4 °C, respectively, suggesting the association of Ru**1** to the third strand (the Hoogsteen base-paired third strand) is tighter than the duplex (the Watson–Crick base-paired duplex) of the triplex. However, for Ru**2**, whose ΔT_{m1} and ΔT_{m2} are about 6.6 and 8.9 °C, respectively, suggesting the binding of Ru**2** with the duplex is stronger than that with the duplex of the triplex. These results suggest specific stabilization of the triplex structure by the two Ru(II) complexes and Ru**1** is a better stabilizer for the triplex in comparison with Ru**2**. Since the intercalative ligands of both complexes are the

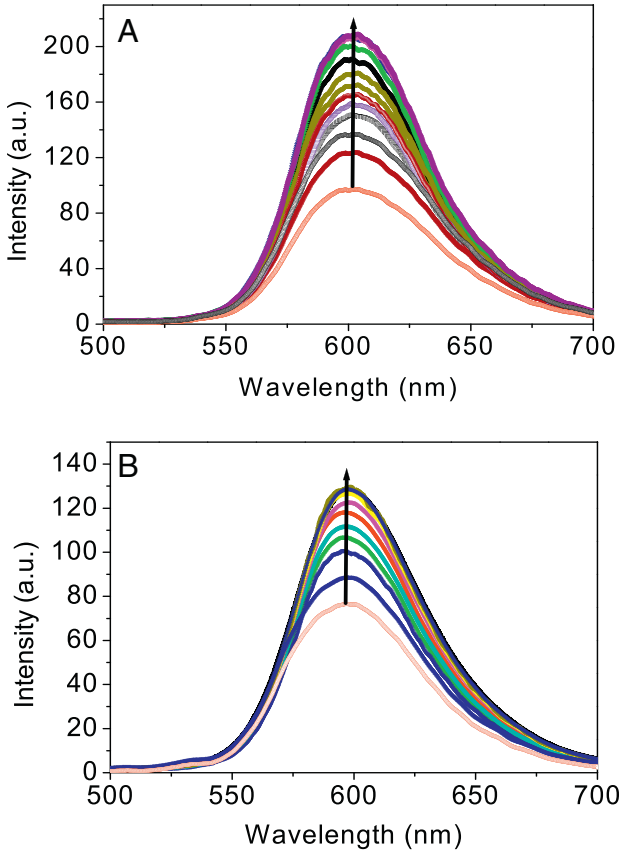

Fig. 6. Representative fluorescence emission spectra of Ru**1** (A) and Ru**2** (B) treated with poly(U)·poly(A)*poly(U). [Ru**1**] = [Ru**2**] = 4.0 μM; for curves 1 → 15 and cures 1 → 10, [UAU] = 0–51.8 μM and 0–33.3 μM, respectively. The arrows show the intensity change upon an increasing poly(U)·poly(A)*poly(U) concentration. Solution conditions are the same as those described in the legend of Fig. 5.

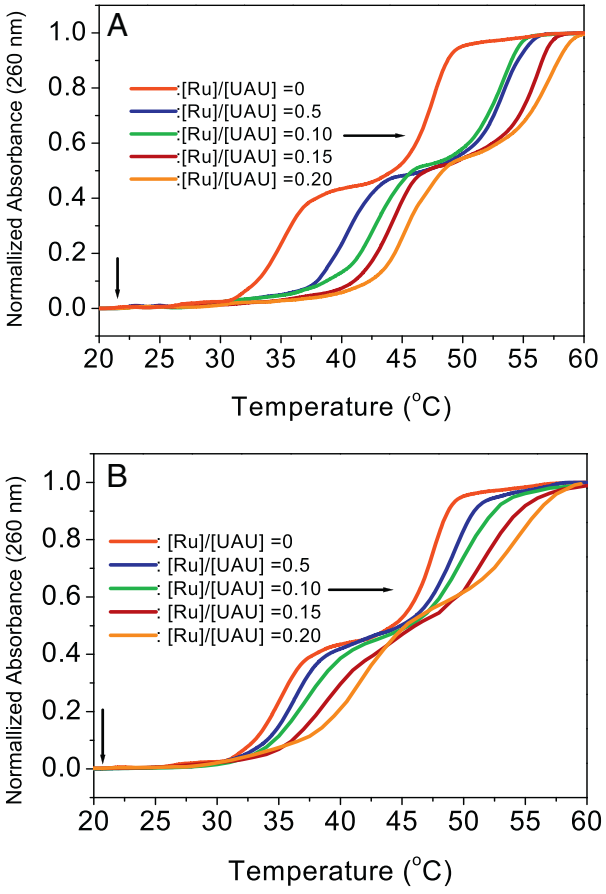

Fig. 7. Melting curves at 260 nm of poly(U)·poly(A)*poly(U) (32.0 μM) and its complexation with Ru**1** (A) and Ru**2** (B) at different C_{Ru}/C_{UAU} ratios. Solution conditions are the same as those described in the legend of Fig. 5, and [Na^+] = 35 mM.

Table 2
Melting Temperature (°C) for poly(U)•poly(A)*poly(U) in the absence and presence of Ru**1** and Ru**2**, respectively. [Na^+] = 35 mM.

Title/complex	C_{Ru}/C_{UAU}	T_{m1} (°C)	$T_{m\,2}$ (°C)	ΔT_{m1}	ΔT_{m2}
poly(U)•poly(A)*poly(U)	0	35.1	47.5	–	–
poly(U)•poly(A)*poly(U) + Ru**1**	0.05	40.2	53.5	5.1	6.0
	0.10	43.0	53.0	7.9	5.5
	0.15	44.0	55.9	8.9	8.4
	0.20	45.6	56.9	10.5	9.4
poly(U)•poly(A)*poly(U) + Ru**2**	0.05	36.5	49.2	1.4	1.7
	0.10	37.2	50.1	2.1	2.6
	0.15	39.1	52.1	4.0	4.6
	0.20	41.7	54.4	6.6	8.9

same, the difference in the RNA stabilization enhanced by Ru**1** and Ru**2** is likely attributed to the ancillary ligand effects. As the ancillary ligand progresses from bpy to phen studied, the bulkiness and hydrophobic character is increased. Consequently, the hydrophobic transfer of the large aromatic complex Ru**1** from solution into the triplex binding site caused by the ancillary ligand phen is more easily to achieve, resulting in the binding sites effectively overlap each other. Therefore, the effect of Ru**1** on the stability of the triplex is more remarkable than that of Ru**2**.

In addition, the effects of the two complexes on the stability of the triplex are significantly different from those of PR and its metal complex PtPR [14], some alkaloids [17] and ethidium [22]. PR and its metal complex PtPR and ethidium were shown to have a destabilizing effect on the Hoogsteen base-paired third strand and a stabilizing effect on the Watson–Crick base-paired duplex, whereas some alkaloids, such as berberine, palmatine and coralyne, could stabilize the Hoogsteen base-paired strand of the triplex without affecting the stability of the Watson–Crick base-paired duplex. These results reveal that the stability of the triplex is very complicated and sensitive to the structural features of the bound small molecule.

3.6. Determination of the binding mode by viscosity studies

To further clarify the interactions between the two complexes and the RNA triplex poly(U)•poly(A)*poly(U), viscosity measurements were carried out by varying [Ru]/[UAU]. The effects of either Ru**1** or Ru**2** on the relative viscosity of the triplex are presented in Fig. 8. It is evident that the binding of either Ru**1** or Ru**2** can increase in the relative viscosity of the triplex solution and a better intercalator may be envisaged for Ru**1** compared with Ru**2**. In addition, the observed decreases in contour length at low loadings may be indicative of a conformational change of the triplex induced by Ru**1** or Ru**2**, while ascribing the subsequent increase in solution viscosity to the effects of intercalation [39]. The results further suggest that the binding modes of Ru**1** and Ru**2** are intercalation [15,17] and Ru**1** binds to the triplex structure more tightly than Ru**2** does, complementing the above results. Notably, the effects of Ru**1** and Ru**2** on the viscosity of the triplex are different from the metal complex PtPR [14]. Concerning PtPR, only a partially intercalated complex can be formed due to the platinum-containing residues prevent full penetration of the PR residue between base planes, which results in no obvious changes of the viscosity of the triplex. These indicate that the size and shape of metal complexes has a significant effect on the modes of metal complexes binding with the triplex.

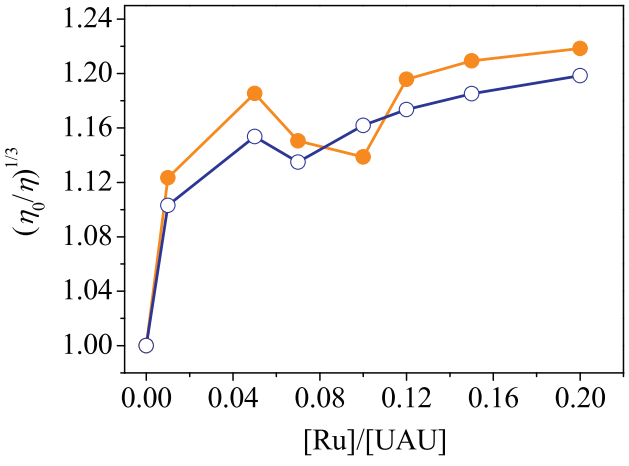

Fig. 8. Viscometric Ru**1** (●) and Ru**2** (○) titrations of poly(U)•poly(A)*poly(U) at 20 °C. [UAU] = 153 μM. Solution conditions are the same as those described in the legend of Fig. 5.

3.7. Comformational transmission studies

The circular dichroic spectrum of the free RNA triplex (Fig. 9A) is characterized by a large positive band at about 260 nm and an adjacent

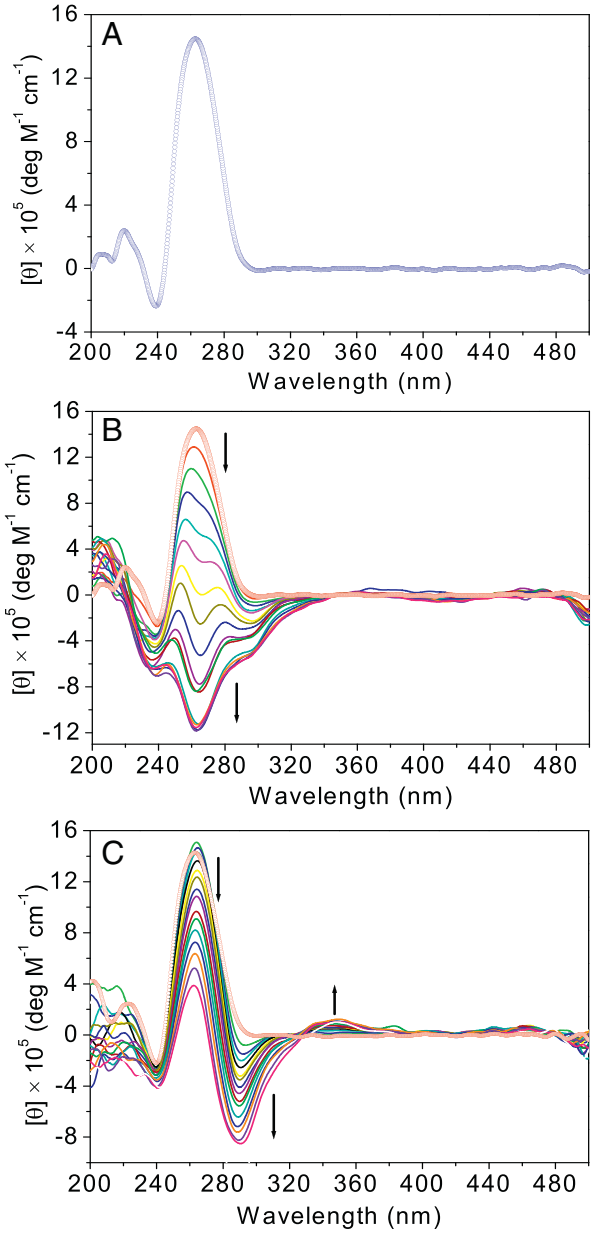

Fig. 9. CD spectra of 100 Mm poly(U)•poly(A)*poly(U) (A) treated with either Ru**1** (B) or Ru**2** (C) at different C_{Ru}/C_{UAU} ratios from 0 to 0.60 or from 0 to 0.64, respectively. The arrows show the change upon an increasing poly(U)•poly(A)*poly(U) concentration. Solution conditions are the same as those described in the legend of Fig. 5.

weak negative band at about 240 nm followed by a small positive band at about 220 nm. These bands are caused most likely due to stacking interactions between the base triplets and the helical structure of the triplex strands and are in conformity with the earlier reports [17]. To investigate the two complexes induced the changes of the conformation of the triplex, we also recorded CD spectra of the triplex RNA modified by Ru**1** (Fig. 9B) and Ru**2** (Fig. 9C). Notably, Ru**1** and Ru**2** have no intrinsic CD signals, as they are racemic compounds so that any CD signals above 300 nm can be attributed to the interaction of the complex with the triplex. Below 300 nm, any changes from the RNA spectrum are due either to the triplex induced CD (ICD) of the metal complex or the metal complex induced perturbation of the triplex spectrum [40]. Binding of Ru**1** to the triplex at low loadings induces strong hypochromic effects on the most energetic band at 263 nm, and then formation of a new negative band centered at around 263 nm, indicating that the triplex undergoes a conformational transition. To the best of our knowledge, Ru**1** is the first example of a small molecular able to induce the triplex conformational transition. In contrast to Ru**1**, binding of Ru**2** to the triplex (Fig. 9C) induces formation of a negative band centered at about 290 nm and a positive band centered at 347 nm, whereas the intrinsic signals of the triplex still survive except that the most energetic band at 260 nm shows obvious hypochromicity. This suggests that the triplex still keeps its helicity in A-type in the presence of Ru**2**. The results also indicate that Ru**1** binds more strongly with the triplex than Ru**2**, which is consistent with the above results.

4. Conclusion

In summary, the binding properties of the RNA triplex poly(U)•poly(A)*poly(U) with Ru**1** and Ru**2** using various biophysical techniques. The studies reveal that the two metal complexes bind to the RNA triplex by intercalation and stabilize the Hoogsteen base-paired third strand. However, the binding affinity of the RNA triplex with Ru**1** is greater than that with Ru**2**. Contrary to Ru**2**, Ru**1** enhancing the stabilization of the Hoogsteen base-paired third strand is stronger than the duplex structure. Furthermore, Ru**1** is able to induce the conformational of the triplex RNA transition, whereas in the case of Ru**2**, the triplex RNA still keeps its helicity in A-type. Considering the structure characteristics of the two metal complexes, we presume that the ancillary ligands have an important effect on third-strand stabilization of the triplex RNA poly(U)•poly(A)*poly(U) when Ru(II) complexes contain the same intercalative ligands. This research further advances our knowledge on the interaction of RNA triple-stranded structures with metal complexes, particularly Ru(II) complexes.

Acknowledgements

We acknowledge the support of the National Natural Science Foundation of China (21371146), Hunan Provincial Natural Science Foundation of China (12JJ2011) and the Key Project of Chinese Ministry of Education (212127).

References

[1] G. Felsenfeld, D.R. Davies, A. Rich, J. Am. Chem. Soc. 79 (1957) 2023–2024.
[2] H.E. Moser, P.B. Dervan, Science 238 (1987) 645–650.
[3] T.L. Doan, L. Perrouault, M. Chassignol, T.T. Nguyen, C.S. Hélène, Nucleic Acids Res. 15 (1987) 8643–8659.
[4] A. Jain, A. Bacolla, P. Chakraborty, F. Grosse, K.M. Vasquez, Biochemistry 49 (2011) 6992–6999.
[5] N.K. Conrad, Wiley Interdiscip. Rev. RNA 5 (2014) 15–29.
[6] A.F. Buske, J.S. Mattick, T.L. Bailey, RNA Biol. 8 (2011) 427–439.
[7] P. Gupta, O. Muse, E. Rozners, Biochemistry 51 (2012) 63–73.
[8] G.N. Ben, Z. Chao, S R. Gerrard, K R. Fox, T. Brown, Chembiochem 10 (2009) 1839–1851.
[9] O. Doluca, A.S. Boutorine, V.V. Filichev, Chembiochem 12 (2011) 2365–2374.
[10] D. Bhowmik, G.S. Kumar, Mol. Biol. Rep. 40 (2013) 5439–5450.
[11] D.P. Arya, Acc. Chem. Res. 44 (2011) 134–146.
[12] D. Bhowmik, S. Das, M. Hossain, L. Haq, G.S. Kumar, PLoS ONE 7 (2012) e37939–e37941.
[13] H.J. Lozano, B. García, N. Busto, J.M. Leal, J. Phys. Chem. B 117 (2013) 38–48; F.J. Hoyuelos, B. García, J.M. Leal, N. Busto, T. Biver, F. Secco, M. Venturinib, Phys. Chem. Chem. Phys. 16 (2014) 6012–6018.
[14] B. García, J.M. Leal, V. Paiotta, R. Ruiz, F. Secco, M. Venturini, J. Phys. Chem. B 112 (2008) 7132–7139.
[15] L.F. Tan, J. Liu, J.L. Shen, X.H. Liu, L.L. Zen, L.H. Jin, Inorg. Chem. 51 (2012) 4417–4419.
[16] L.F. Tan, L.J. Xie, X.N. Sun, J. Biol. Inorg. Chem. 18 (2013) 71–80.
[17] R. Sinha, G.S. Kumar, J. Phys. Chem. B 113 (2009) 13410–13420.
[18] H.J. Xi, E. Davis, N. Ranjan, L. Xue, D. Hyde-Volpe, D.P. Arya, Biochemistry 50 (2011) 9088–91113.
[19] A.K. Shchyolkina, E.N. Timofeev, Y.P. Lysov, V.L. Florentiev, T.M. Jovin, D.J. Arndt-Jovin, Nucleic Acids Res. 29 (2001) 986–995.
[20] M. Polak, N.V. Hud, Nucleic Acids Res. 30 (2002) 983–992.
[21] E.A. Lehrman, D.M. Crothers, Nucleic Acids Res. 4 (1977) 1381–1392.
[22] B. Garcia, J.M. Leal, V. Paiotta, S. Ibeas, R. Ruiz, F. Secco, M. Venturini, J. Phys. Chem. B 110 (2006) 16131–16138.
[23] S. Delaney, J. Yoo, E.D.A. Stemp, J.K. Barton, Proc. Natl. Acad. Sci. U. S. A. 101 (2004) 10511–10516.
[24] J.C. Genereux, J.K. Barton, Chem. Rev. 110 (2010) 1642–1662.
[25] A.R. Arnold, J.K. Barton, J. Am. Chem. Soc. 135 (2013) 15726–15729.
[26] S. Satyen, S. Anunay, J. Phys. Chem. A 106 (2002) 4763–4771.
[27] R.B. Elmes, M. Erby, S.A. Bright, D.C. Williams, T. Gunnlaugsson, Chem. Commun. 48 (2012) 2588–2590.
[28] R.M. Duke, E.B. Veale, F.M. Pfeffer, P.E. Kruger, T. Gunnlaugsson, Chem. Soc. Rev. 39 (2010) 3936–3953.
[29] S. Banerjee, E.B. Veale, C.M. Phelan, S.A. Murphy, G.M. Tocci, L.J. Gillespie, D.O. Frimannsson, J.M. Kelly, T. Gunnlaugsson, Chem. Soc. Rev. 42 (2013) 1601–1618.
[30] S. Banerjee, J.A. Kitchen, S.A. Bright, J.E. O'Brien, D.C. Williams, J.M. Kelly, T. Gunnlaugsson, Chem. Commun. 49 (2013) 8522–85524.
[31] M. Yamada, Y. Tanaka, Y. Yoshimato, S. Kuroda, I. Shimao, Bull. Chem. Soc. Jpn. 65 (1992) 1006–1011.
[32] H.L. Hwang, Y.J. Liu, C.H. Tseng, L.X. He, F.H. Wu, DNA Cell Biol. 29 (2010) 261–270.
[33] B.P. Sullivan, D.J. Sullivan, T.J. Meyer, Inorg. Chem. 17 (1978) 3334–3341.
[34] V. Buckin, H. Tran, V. Morozov, L.A. Marky, J. Am. Chem. Soc. 118 (1996) 7033–7039.
[35] S. Das, G.S. Kumar, A. Ray, M. Maiti, J. Biomol. Struct. Dyn. 20 (2003) 703–714.
[36] M.T. Carter, M. Rodriguez, A. Bard, J. Am. Chem. Soc. 111 (1989) 8901–8911.
[37] Y. Xiong, X.F. He, X.H. Zou, J.Z. Wu, X.M. Chen, L.N. Ji, R.H. Li, J.Y. Zou, K.B. Yu, Dalton Trans. (1999) 19–23.
[38] S. Zails, V. Drchal, Chem. Phys. 118 (1987) 313–317.
[39] S.D. Choi, M.S. Kim, S.K. Kim, P. Lincoln, E. Tuite, B. Nordén, Biochemistry 36 (1997) 214–223.
[40] A. Kabir, G.S. Kumar, Mol. BioSyst. 10 (2014) 1172–1183.
[41] P.V. Scaria, R.H. Shafer, J. Biol. Chem. 266 (1991) 5417–5423.
[42] B. Tijana, N. Olga, H. Anna, Z. Lenka, V. Oldrich, K. Jana, H. Abraha, P. Simon, J.S. Peter, B. Viktor, J. Med. Chem. 51 (2008) 5310–5319.